Advances in Applied Sciences
2019; 4(5): 97-103
http://www.sciencepublishinggroup.com/j/aas
doi: 10.11648/j.aas.20190405.11
ISSN: 2575-2065 (Print); ISSN: 2575-1514 (Online)

Effects of Microcavity Local Resonators on the Bandgap Characteristics of a Two-Dimensional Phononic Crystal Structure

Randy Amuaku[1, *], Wen Huabing[2], Eric Amoah Asante[1], Augustus Buckman[2]

[1]Koforidua Technical University, Faculty of Engineering, Koforidua, Ghana

[2]Jiangsu University of Science and Technology, School of Energy and Power, Zhenjiang, China

Email address:

amuaku.randy@ktu.edu.gh (R. Amuaku)

[*]Corresponding author

To cite this article:

Randy Amuaku, Wen Huabing, Eric Amoah Asante, Augustus Buckman. Effects of Microcavity Local Resonators on the Bandgap Characteristics of a Two-Dimensional Phononic Crystal Structure. *Advances in Applied Sciences.* Vol. 4, No. 5, 2019, pp. 97-103.
doi: 10.11648/j.aas.20190405.11

Received: October 5, 2019; **Accepted**: October 25, 2019; **Published**: November 8, 2019

Abstract: The emergence of acoustic metamaterials generated a lot of attention in the study of low-frequency vibration, noise control and reduction in engineering applications. As a result, the elastic wave bandgap characteristics of a two-dimensional microcavity local resonator structure for two soft rubber materials was investigated using finite element methods (FEM). The transmission spectrum of the displacement eigenmodes of the bandgap edges relating to the lowest bandgap was calculated. The results showed that the phononic crystal structure without a microcavity local resonator plate has bandgap characteristics of elastic wave propagation in the high-frequency range between 2200~2400Hz. However, with the introduction of microcavity resonator plates in the phononic crystal structure low-frequency bandgaps are obtained in the region of 0~198Hz and 0~200Hz respectively. The low-frequency bandgaps appeared as a result of the microcavity local resonator plate which increased the path length through which the wave is transmitted. The phononic crystal microcavity local resonator plate structure has varying transmission loss characteristics of -65dB, -85dB, -100dB and -150dB in the low-frequency range depending on the number of local resonator plates introduced into the cell structure and density of the cell structure. The study provided a good demonstration of wave propagation in artificially engineered materials with critical emphasis on the effects of local resonators in a microcavity structure.

Keywords: Bandgap Characteristics (BGs), Microcavity Phononic Crystal (MPCs), Finite Element Method (FEM), Perfectly Matched Layer (PML), Local Resonator Plate Structure (LRPS)

1. Introduction

In recent years, huge attention has been focused on the study of artificially engineered materials known as phononic crystal acoustic metamaterials. Many of the studies centered on the propagation and control of elastic and acoustic waves in periodic and non-periodic structures [1, 2]. Phononic Crystal structures composed of two or more materials with different mechanical properties such as density and modulus of elasticity which leads to bandgaps (BGs) generation during the transmission of elastic or acoustic waves [3, 4]. Phononic crystal materials have rich physical properties and an enormous potential application in the design of acoustic devices for the control and reduction of the effects on low-frequency vibration and noise [5, 6]. The bandgap structure is expressed as the dispersion of the elastic waves in the infinite periodic phononic crystal, which can be clearly defined by the band structure analysis. To control and reduce the effects of vibration and noise in engineering structures and components, it is of great importance to obtain bandgaps with large bandwidth in low-frequency ranges [7, 8]. Bandgap widths can be enlarged by exploiting rainbow-trapping designs [9], topology optimization techniques [10] or coupling the Bragg and local resonant mechanisms [11]. Over the past decade, researchers have developed structures which yield large bandgaps with good wave propagation characteristics in the low-frequency range. For instance, Jia., et al, [12] carried out a study on a phononic crystal structure which composed of a

square lattice of steel cylinders arranged in air and found that the bandgaps could be tunable with various microstructures. In another study Liu., et al, introduced narrow-slit structures into a two-dimensional phononic structure, which composed of steel tubes placed in air and obtained large bandgaps inaudible frequency range [13, 14]. In order to show the existence of bandgaps in two orders of magnitude smaller than the relevant wavelength, Liu, et al designed and evaluated a three-component phononic crystal structure and proposed a localized resonance (LR) mechanism [15]. However, Local resonant phononic crystal structures show low-frequency bandgaps without taking into consideration the size of the structure. Acoustic metamaterials exploit local resonances to induce low-frequency band gaps which allows the control of waves at much larger wavelengths than their microstructural scales [16, 17]. In order to assess the effects of local resonance on bandgaps formation in structures, Brunet et al. [18], used a silicon slab made of centered rectangular and square array of holes, and reported that there was no complete bandgap. Similarly, Gao., et al, identified full bandgap for surface acoustic waves in a piezoelectric phononic crystal composed of a square-lattice Y-cut lithium niobate matrix with circular void inclusions [19]. The local resonance effect is induced by coated inclusions or pillars, increasing the total structural weight. In recent times, extensive research has revealed some novel periodic structures with a large bandgap width [20]. For instance, Manktelow, et.al [21] studied the nonlinear periodic materials and Sigmund et.al reported [22] large bandgap shifts in one and two dimensions via optimal topologies. Hsu. et al [23] conducted research on a two-dimensional phononic crystal with neck structure inclusions and phononic crystal slabs with periodic stepped resonators and obtained large bandgaps in the low frequency range. Based on literature reviewed, it is now clear that local resonance plays an important role in bandgap formation. However, there is limited information on the effects of the number of local resonators on the bandgap in a phononic crystal structure. Therefore, this paper seeks to: (1) design a square lattice scatter attached with a varying number of local resonator plates which forms a microcavity to assess bandgap characteristics. (2) study the effect of the number of local resonators in two-dimensional phononic crystal structure for two soft rubber materials. (3) propose and find the application of the model structure in controlling low-frequency elastic and acoustic wave propagation in engineering structures using finite element method in a wide range of frequencies. The array cell and unit cell structures of the microcavity phononic crystal is presented in Figure 1 below,

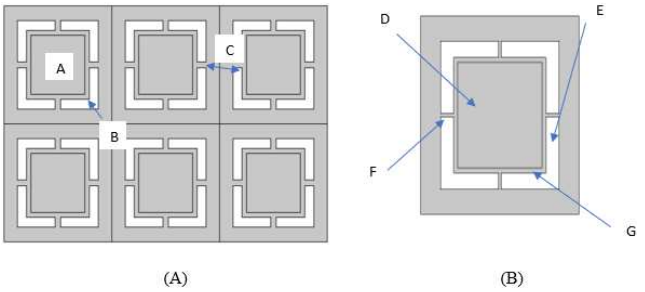

Figure 1. *(3*2) Array phononic crystal structure (A) and Unit cell phononic crystal structure (B).*

2. Methodology

Model and Bandgap Calculation Method

The phononic crystal cell structure proposed for the analysis of the bandgap characteristics comprises of a square lattice scatter with four inclusion plates uniformly attached to opposite sides of the square scatter. The schematic view of the array and unit cell structures is presented in Figure 1. The alphabets A, B, C, D E, F and G represent the soft rubber materials, square scatter, air domain, solid domain and local resonator plates respectively. The infinite system is formed by repeating the length and breadth of the unit cell $a_1 = a_2 = 12mm$ periodically along the X~Y directions simultaneously to form a uniform array pattern. The outside and inside diameter of the square scatter and the local resonator plate diameters are *D*=6.8*mm, E*=9*mm*, *G*=7*mm* and *F*=0.25*mm* respectively. The phononic crystal structure is surrounded by vacuum therefore its dispersion relation in an infinite system is considered and calculated. A control equation for the propagation of an elastic wave in a solid structure is applied,

$$\sum_{j=1}^{3} \frac{\partial}{\partial x_j} \left(\sum_{i=1}^{3} \sum_{k=3}^{3} C_{ijkl} \frac{\partial u_k}{\partial x_l} \right) = \rho \frac{\partial^2 u_i}{\partial t^2} (i = 1, 2, 3) \tag{1}$$

Where, ρ is the mass density, C_{ijkl} is the elastic constant, u_i is the displacement, t is time, $x_j (j = 1, 2, 3)$ corresponds to the coordinate variable x, y and z respectively. The infinite system is arranged periodically in the X and Y direction, making it easier to apply a Blotch-Floquet periodicity to the boundaries of the unit cell structure. Through the application of periodicity on the unit cell structure, the wave propagation characteristics can be determined by introducing periodic boundary conditions along the X~Y direction. The wave vector parameter k is introduced into the periodic boundary condition within the first irreducible Brillouin boundary of the unit cell structure to solve the eigenvalues of the spectra problem which describes the wave propagation characteristics of the whole phononic crystal structure. The bandgap characteristics are calculated using the unit cell structure. The study on the unit cell makes it easy to analyze the behavior of the structure and its characteristics in relation to elastic and acoustic wave propagation. As a result of the application of the finite element method (FEM), the Blotch periodic boundary condition is applied to the boundaries of the unit cell,

$$u(r + a) = e^{i(k*a)} u(r) \tag{2}$$

Where r is the boundary nodes, k is the wave vector, u is the displacement at the nodes and a is the vector which generates the point lattice associated with the phononic crystal structure. The dispersion curves are built by varying the wave vector $k = (k_x, k_y)$ along the first Brillouin zone for a given propagation direction. For the analysis of the transmission spectra, the bandgap characteristics of the structure are calculated using different unit cell structure arrangement. The different structural arrangement is based on the inclusion of local resonator plates in the unit cell. In order to investigate the effects of the local resonator plates on the bandgap characteristics of the microcavity phononic crystal structure, a unit cell structure with no resonator, single resonator, double resonator, triple resonator and a quadruple resonator is studied. The number of local resonator plates forming the microcavity has effects on the bandgap characteristics in relation to the bandwidth within the upper and lower edges of the wave propagation.

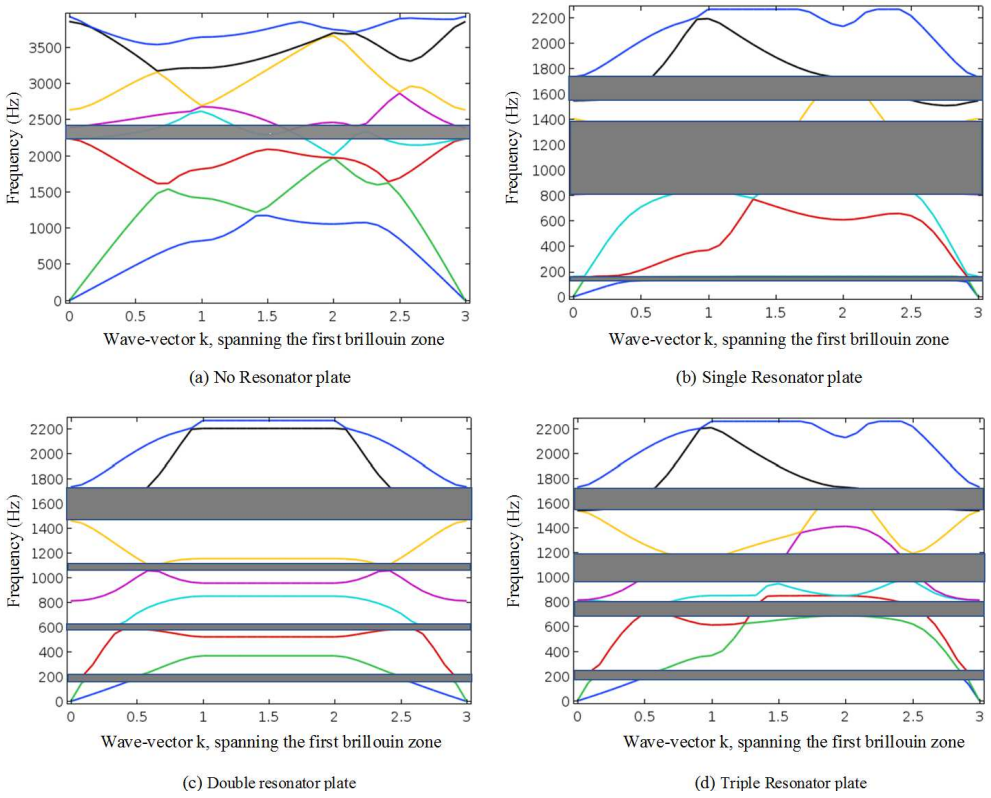

Figure 2. *Bandgap characteristics of a structure with (a) No Resonator, (b) Single Resonator, (c) Double resonator and (d) Triple Resonator.*

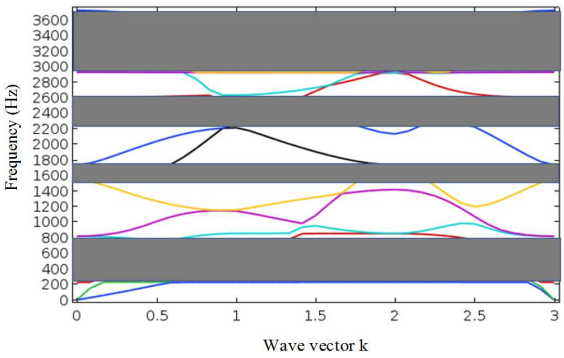

Figure 3. *Bandgap Characteristics of a structure with Quadruple Resonator plates.*

3. Results and Discussion

3.1. Bandgap Characteristics

The results of the wave propagation in the structure are presented in Figures 2 and 3 respectively. The formation of bandgap characteristics of the unit cell structure occurs as a result of elastic wave propagation effects in the periodic structure under Blotch Floquet periodicity boundary conditions. They are formed when the phononic crystal structure reacts to elastic wave deformations. The torsion and deformations of the structure represent the bandgap characteristic width. The color maps show the various characteristics in relation to the modes of deformation of the unit cell structure under various elastic wave propagation frequencies using the solid mechanics structure module of Comsol Multiphysics software 5.3a. The model shapes represent the torsion of the resonators and the elastic wave propagation within the structure at different frequency range.

3.1.1. Modal Shapes of Bandgap Structure

In order to analyze the transmission spectra of the structure, a finite system is defined. The phononic crystal structure is considered as finite in the x-direction with X number of units defined. In the y-direction, Y number of units is also defined to complete the infinite cell structure. In applying the units ($X * Y$) in the x-y direction a finite array structure is formed which is calculated using Comsol

Multiphysics 5.3a. Plane excitation waves are applied through an acceleration excitation source from one end of the array structure in the x-direction. The wave transmission is recorded at the other side of the array structure. The transmission characteristics is defined as,

$$TL = 20\log\left(\frac{w_o}{w_i}\right) \tag{3}$$

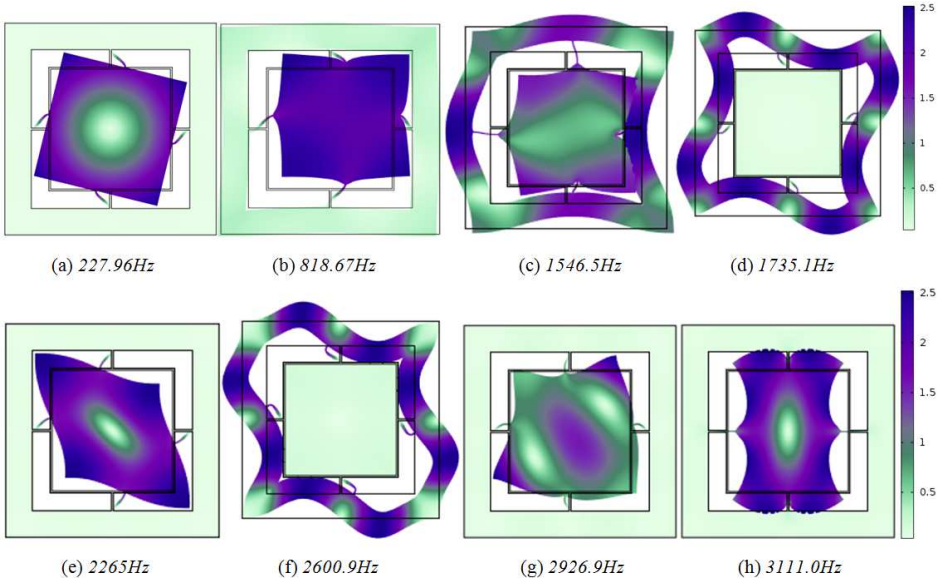

Figure 4. *Modal shapes of the first eight frequency bands of the bandgap structure in Figure 3.*

Where, w_o and w_1 are the values of the transmitted and incident acceleration sources respectively. In varying the excitation frequency at the incident source, the wave transmission spectra can be obtained. The material for the outer plate membrane is silicone rubber and the core square scatter is Epoxy resin. The material parameters for silicone rubber are as follows: density $\rho_1 = 4.08kg/m^3$, young's modulus of elasticity $E_1 = 11600P_a$ and Poisson's ratio $V_1 = 0.369$. The material parameters for Epoxy resin are as follows: density $\rho_2 = 0.435kg/m^3$, young's modulus of elasticity $E_2 = 1180P_a$ and Poisson's ratio $V_2 = 0.370$.

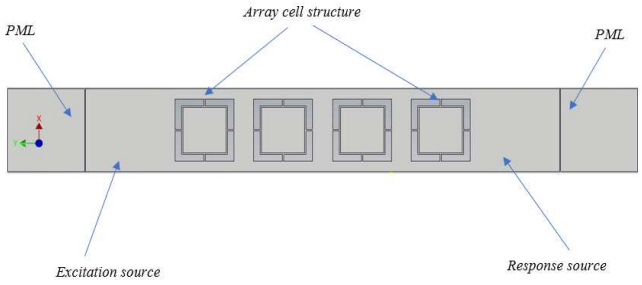

Figure 5. *Array structure for the Transmission Analysis.*

The transmission spectra were calculated using four primary cell structures in the longitudinal direction. In Comsol Multiphysics 5.3a. Figure 5 is set up with other layers to form a (4*4) array structure in the vertical and horizontal directions. The perfectly matched layers are placed at opposite ends of the array structure to prevent reflection of waves during propagation. The transmission spectra were calculated within the perfectly matched layer structure attached to both ends of the array structure. A background field layer is placed between the excitation source and the array structure to control the flow of waves through the array structure. An excitation of 2mm is given at the excitation source, the wave propagation transmission characteristics of the structure are obtained at the response source and the transmission loss is also obtained accordingly. The wave transmission loss characteristics of the microcavity local resonator phononic crystal structure is calculated using a (4*4) array unit cell arrangement. The results of the transmission loss characteristics are shown in Figures 6 and 7.

3.1.2. Transmission Loss Characteristics

The transmission loss characteristics of the cell structure with four resonators show sharp transmission loss dips at frequencies -65dB and -85dB. The transmission loss dips are very sharp as a result of the width of the quadruple resonator plates placed at the opposite sides of the square scatter in the unit cell structure. There were several sharp dips which refer to high attenuation efficiency in the transmission spectra of the periodic structures with the inclusion of local resonators. The increase in the number of unit cells for the transmission characteristics is also found to enhance the attenuation efficiency. However, a transmission loss dip with a broad width was observed in the frequency range of 1000Hz~1500Hz at a transmission loss of -20dB (Figure 6). The transmission loss characteristics of the quadruple array structure are in good agreement with the bandgap characteristics of the quadruple resonator unit cell structure. The structure showed a low-frequency bandgap of 200~800Hz whiles the first transmission loss dip is observed in a frequency range of 500~600Hz (Figure 7). Transmission

loss characteristics for four different cell structures arranged in an array of (4*4) along the x y direction respectively was calculated. The various structures show transmission loss characteristics at varying frequency ranges. The four local resonators structure however, shows high transmission loss characteristics within low-frequency ranges which is good for elastic wave control and conforms with the findings of Mao Liu et.al [23].

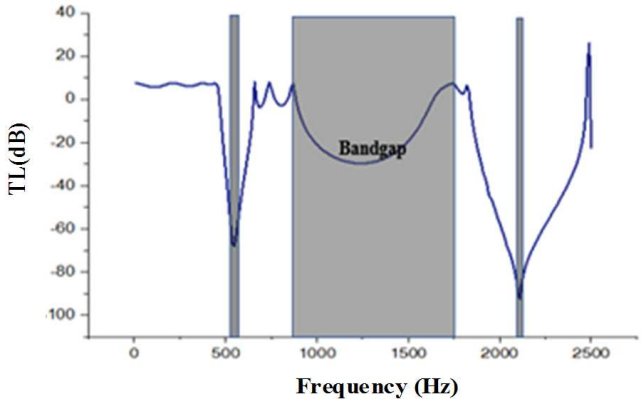

Figure 6. *Transmission loss for Quadruple local resonator structure.*

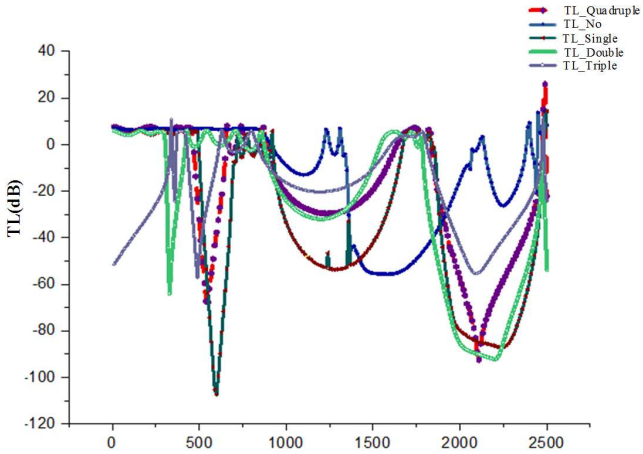

Figure 7. *Transmission loss Characteristics of a No resonator, Single, Double, Triple and Quadruple Resonator Structure.*

The analysis of the transmission characteristics of the microcavity local resonator phononic crystal structure with different number of resonators showed sharp transmission loss dips in the low-frequency range of 0~600Hz with transmission loss dips around -63dB, -65dB and -110dB. However, from frequencies of 1000~1600Hz, the width of the transmission loss dips is broad but have low dip losses in the range of 0dB to -45dB. The transmission loss characteristics increased further from -80dB to -85dB within frequency range of 2000~2500Hz (Figure 7). The bandgap and the transmission loss characteristics were very low as compared to the findings of Mao Liu et.al due to the differences in the thickness and the number of the resonator plates present. In the low-frequency range the bandgap characteristics in the unit cell structure decreases with the increase in resonator plates. Furthermore, the transmission loss characteristics determined on an array structure arranged in (4*4) matrix for multiple resonator plates structure is the best for optimum transmission. The transmission loss characteristics for the various structures agree with the bandgap characteristics in Figures 2 and 3 respectively. The low-frequency ranges for the transmission loss characteristics make the microcavity local resonator phononic structure an idea structure for vibration and noise control in engineering applications and structures.

3.2. Effects of Local Resonators on the Bandgap Characteristics

The effects of the local resonator plates on the bandgap characteristics was investigated. It is seen clearly that the structure with no local resonator plate has a bandgap characteristic at a high-frequency range of 2200~2400Hz with broad upper and lower bandwidth (Figure 2a). However, with the introduction of a single resonator within the unit cell structure, a low-frequency bandgap is opened at a frequency range of 0~198Hz (Figure 2b). Although the bandgap is opened within the low-frequency range the bandwidth is reduced compared to the bandwidth of the structure with no resonator plate. Subsequently, with the introduction of a double resonator plate within the unit cell structure, the bandgap increased to 200Hz but still within the low-frequency range. However, the subsequent bandgaps are opened at frequency range of 200~1100Hz. The upper and lower edges of the bandgap width are narrow compared to the bandwidth of the unit cells with no resonator and single resonator. For the upper edge of the bandgap widths, an increase in the resonator plate width causes an increase in the stiffness of the resonator plates within the mass-spring system leading to the occurrence of resonance frequency bandgaps. The unit cell structures with triple and quadruple resonator plates however have bandgaps within 0~200Hz and 200~800Hz respectively (Figure 2c and 2d). The upper and lower edges of the bandwidth in both cell structures are much broader compared to the edges of the subsequent bandgap. The overall trend showed that the higher the number of local resonator plates introduced into the unit cell structure the better the transmission loss characteristics.

3.3. Effects of Local Resonator Plates on the Transmission Loss Characteristics

The transmission loss characteristics of five models comprising of unit cell structures with No resonator plate, single resonator plate, double resonator plate, triple resonator and quadruple resonator plates are presented in Figure 7. The introduction of the local resonators into the unit cell structure and its width had an effect on the transmission loss characteristics. The analysis clearly showed that all the cell structures have transmission losses within a low-frequency range of 0~600Hz except the structure with no resonator plate (Figure 7). This is because an increase in the number of local resonators has a direct correlation on the increase of the bandgaps which increases the path length through which the elastic wave is transmitted. Using a local resonator width of $F = 0.25mm$ thickness (Figure 1b) has improved the

transmission efficiency by reducing the transmission loss characteristics with emphasis on the narrow transmission dips shown in the cell structures with local resonator plates. Furthermore, high attenuation efficiency in the transmission spectra of the periodic structures with the inclusion of resonator plates was achieved.

3.4. Effects of Density on the Cell Structure and Local Resonators in Relation to Transmission Loss Characteristics

In order to verify the effects of density on the transmission loss characteristics, the width of the local resonator is increased to $2.0mm$. The density of the materials is also increased. The density of Silicone rubber $\rho_1 = 4.08kg/m^3$ is increased to $12kg/m^3$, Epoxy resin material density of $\rho_2 = 0.435kg/m^3$ is increased to $10kg/m^3$. The increase in density of the material causes an increase in the transmission characteristics spectra which is reflected in attenuation frequency dips (Figure 8).

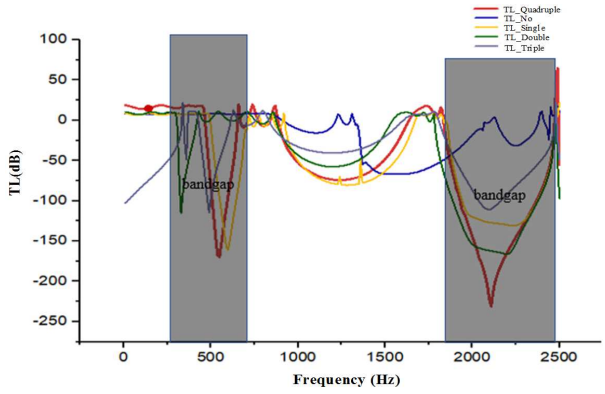

Figure 8. *Effects of density of material on Transmission loss Characteristics.*

The cell structure with resonators had increased transmission losses with sharp transmission dips and high attenuation frequency. The simulation results for various cell structures had improved transmission loss dips. Further increase in density of the structure may not necessarily reduce the minimum transmission of the structure but can improve the transmission dips which is of huge importance in controlling vibration in engineering application and structures. The unit cell structure with four resonator plates had good sharp transmission attenuation dips of -155dB at $508Hz$ and -210dB at $2125Hz$ frequencies (Figure 8).

4. Conclusion

In conclusion, the bandgap characteristics and transmission loss characteristics of a microcavity local resonator phononic crystal structure for two materials have been evaluated using finite element methods (FEM). The study revealed that the bandgap characteristics can be opened in the low-frequency ranges when local resonators are introduced into the unit cell structure. The transmission loss characteristics showed that the local resonator width, number and density of material has effects on the transmission loss dips. In summary, the following conclusions can be made based on the study of the proposed model structure,

i. The bandgap of the acoustic microcavity local resonator, phononic structure model in this study has low-frequency bandgaps at 0~198Hz and 0~200Hz with the inclusion of local resonators but has high-frequency bandgap at 2200~2400Hz without the inclusion of a local resonator.
ii. The structure with four resonators had the lowest frequency bandgap and transmission loss characteristics which is good for controlling elastic waves propagation.
iii. The number of periodic resonator structures of the finite periodic array structure can be increased, and more attenuating elastic bandgaps can be obtained in the low-frequency range.
iv. The results of the study make the microcavity local resonator phononic crystal structure an ideal structure which when further researched and practically applied can be used in low to high-frequency vibration and acoustic engineering applications.

The study provided a good demonstration of wave propagation in artificially engineered materials with critical emphasis on the effects of local resonators in a microcavity structure. Further studies will focus on the thickness of the resonators and performing experiments on the structure to determine its practical application in elastic and acoustic wave propagation.

Acknowledgements

The authors wish to acknowledge that this research work was founded by the Academic Research Department of Koforidua Technical University in collaboration with Vibration and Noise control Engineers from the school of Energy and Power Engineering in Jiangsu University of Science and Technology.

References

[1] Xiao, Y., J. Wen, and X. Wen, Longitudinal wave band gaps in metamaterial-based elastic rods containing multi-degree-of-freedom resonators. New Journal of Physics, 2012. 14 (3): p. 033042.

[2] Li, J.-B., Y.-S. Wang, and C. Zhang, Tuning of acoustic bandgaps in phononic crystals with Helmholtz resonators. Journal of Vibration and Acoustics, 2013. 135 (3): p. 031015.

[3] Zhang, Y., L. Han, and L. h. Jiang, Transverse vibration bandgaps in phononic crystal Euler beams on a Winkler foundation studied by a modified transfer matrix method. physica status solidi (b), 2013. 250 (7): p. 1439-1444.

[4] Assouar, M. B., et al., Hybrid phononic crystal plates for lowering and widening acoustic band gaps. Ultrasonics, 2014. 54 (8): p. 2159-2164.

[5] Yang, S., et al., Focusing of sound in a 3D phononic crystal. Physical review letters, 2004. 93 (2): p. 024301.

[6] Wagner, M. R., et al., Two-dimensional phononic crystals: Disorder matters. Nano letters, 2016. 16 (9): p. 5661-5668.

[7] Baravelli, E. and M. Ruzzene, Internally resonating lattices for bandgap generation and low-frequency vibration control. Journal of Sound and Vibration, 2013. 332 (25): p. 6562-6579.

[8] Claeys, C. C., et al., On the potential of tuned resonators to obtain low-frequency vibrational stop bands in periodic panels. Journal of Sound and Vibration, 2013. 332 (6): p. 1418-1436.

[9] Matlack, K. H., et al., Composite 3D-printed metastructures for low-frequency and broadband vibration absorption. Proceedings of the National Academy of Sciences, 2016. 113 (30): p. 8386-8390.

[10] Krushynska, A. O., et al., Accordion-like metamaterials with tunable ultra-wide low-frequency band gaps. arXiv preprint arXiv: 1804.02188, 2018.

[11] Krushynska, A., et al., Coupling local resonance with Bragg band gaps in single-phase mechanical metamaterials. Extreme Mechanics Letters, 2017. 12: p. 30-36.

[12] Jia, Z., et al., Designing Phononic Crystals with Wide and Robust Band Gaps. Physical Review Applied, 2018. 9 (4): p. 044021.

[13] Korozlu, N., et al., Acoustic Tamm states of three-dimensional solid-fluid phononic crystals. The Journal of the Acoustical Society of America, 2018. 143 (2): p. 756-764.

[14] Liu, M., J. Xiang, and Y. Zhong, The band gap and transmission characteristics investigation of local resonant quaternary phononic crystals with periodic coating. Applied Acoustics, 2015. 100: p. 10-17.

[15] Cummer, S. A., J. Christensen, and A. Alù, Controlling sound with acoustic metamaterials. Nature Reviews Materials, 2016. 1 (3): p. 16001.

[16] Christensen, J., et al., Vibrant times for mechanical metamaterials. Mrs Communications, 2015. 5 (3): p. 453-462.

[17] Brunet, T., et al., Lamb waves in phononic crystal slabs with square or rectangular symmetries. 2008. 104 (4): p. 043506.

[18] Gao, N., J. H. Wu, and L. J. U. Yu, Research on bandgaps in two-dimensional phononic crystal with two resonators. 2015. 56: p. 287-293.

[19] Lu, Y., et al., 3-D phononic crystals with ultra-wide band gaps. Scientific reports, 2017. 7: p. 43407.

[20] Manktelow, K. L., M. J. Leamy, and M. Ruzzene, Topology design and optimization of nonlinear periodic materials. Journal of the Mechanics and Physics of Solids, 2013. 61 (12): p. 2433-2453.

[21] Sigmund, O. and J. S. Jensen, Systematic design of phononic band–gap materials and structures by topology optimization. Philosophical Transactions of the Royal Society of London A: Mathematical, Physical and Engineering Sciences, 2003. 361 (1806): p. 1001-1019.

[22] Hsu, J.-C. J. J. o. P. D. A. P., Local resonances-induced low-frequency band gaps in two-dimensional phononic crystal slabs with periodic stepped resonators. 2011. 44 (5): p. 055401.

[23] Liu, M., et al., Research on the band gap characteristics of two-dimensional phononic crystals microcavity with local resonant structure. 2015. 2015.